Proc. Natl. Acad. Sci. USA
Vol. 90, pp. 6904–6908, August 1993
Applied Mathematics

Discrete and integral Fourier transforms: Analytical examples

(signal processing/Gibbs phenomenon)

WILLIAM J. THOMPSON AND J. ROSS MACDONALD

Department of Physics and Astronomy, University of North Carolina, Chapel Hill, NC 27599-3255

Contributed by J. Ross Macdonald, January 28, 1993

ABSTRACT **Analytical examples of the discrete Fourier transform (DFT) help in understanding relations between the DFT and the Fourier integral transform (FIT). Such examples enable one to estimate the errors involved when one transform is approximated by the other, and they suggest how such approximation errors might be reduced. We present mathematical and numerical analyses of the time-to-frequency DFT of the complex exponential function and of the frequency-to-time inverse DFT of the relaxation function. The FITs of these functions are exact inverses, and so they serve to clarify the effects of aliasing and truncation on the DFT.**

1. Introduction

Thorough understanding of Fourier transforms is important in many areas of applied mathematics. Particularly significant are distinctions between Fourier integral transforms (FITs) and discrete Fourier transforms (DFTs). For many functions the FIT can be calculated analytically, but the DFT can seldom be so expressed. On the other hand, since applications are made to discrete data, a DFT is usually appropriate for numerical work because the fast Fourier transform (FFT) may be used to compute the DFT efficiently (1–7). It is therefore important to understand the conditions under which the DFT and FIT produce results close enough for all practical purposes, and to study the effects of aliasing (undersampling) and truncation (finite sample length) in a DFT.

Although there are hundreds of readily calculated integral transforms, the only analytical examples of the discrete transform that we found in about 50 texts and monographs (e.g., refs. 1–6 and 8) were for the rectangular pulse and the train of spikes, which are not typical of real-world problems. We discovered two realistic examples that can be transformed simply and analytically for both the DFT and the FIT—namely, the (truncated) complex-exponential function and the function that is its integral transform, often called the relaxation function (akin to the Lorentzian and Debye functions). The first example is presented in a text on computing (7), but the second has not been published.

We use the language of digital signal processing, since discrete and integral transforms are discussed most extensively in this field. The same considerations apply in several other fields, such as digital image processing. Our notation is generally that of Brigham (2). In particular, we write $j = \sqrt{-1}$, usually denoted by i in mathematics.

2. Time-to-Frequency Transform of the Complex Exponential

The first function we Fourier transform is defined in the time domain as $h(t)$, the complex exponential for $t \geq 0$,

$$h(t) = e^{-\alpha t}, \qquad \text{Re } \alpha > 0 \qquad [1]$$

and zero for $t < 0$. The condition on α ensures convergence for positive t when the number of points in the transform, N, is increased indefinitely to obtain the integral transform. Apart from the inclusion of (complex) α, we are investigating analytically the worked numerical example in chapter 9.1 of Brigham (2).

Analysis of the transform. We use Brigham's notation for the DFT of Eq. **1**. The DFT over N points with time step Δt (Brigham's T) we write, following equation 9.1 of Brigham,

$$H_N(n) = \Delta t\left[\left(\sum_{k=0}^{N-1} e^{-\alpha k\Delta t}e^{-j\omega k\Delta t}\right) - \frac{1}{2}\right], \qquad [2]$$

in which the frequency variables ω and f are related to n by

$$\omega = \frac{2\pi n}{N\Delta t}, \qquad f = \frac{n}{N\Delta t}. \qquad [3]$$

Eq. **2** differs slightly from the usual DFT by the overall factor Δt, which ensures convergence to the Fourier integral for large N as $\Delta t \to 0$. The subtracted term in Eq. **2** ensures correctness of the inverse transform by removing half the value at the point of discontinuity, $k = 0$, as discussed in ref. 2. The sum in Eq. **2** is a geometric series with multiplier

$$r = e^{-(\alpha+j\omega)\Delta t}, \qquad [4]$$

so the series is

$$\sum_{k=0}^{N-1} r^k = \begin{cases} \dfrac{1-r^N}{1-r} & r \neq 1 \\ N & r = 1. \end{cases} \qquad [5]$$

The DFT of the complex exponential Eq. **1** is therefore

$$H_N(n) = \Delta t\left[\frac{1-e^{-\alpha N\Delta t}}{1-e^{-\alpha\Delta t-2\pi jn/N}} - \frac{1}{2}\right] \qquad [6]$$

unless the product of the exponents in the denominator is unity, when

$$H_N(n) = \Delta t\left[N - \frac{1}{2}\right]. \qquad [7]$$

This is also the value obtained by applying L'Hôpital's rule to Eq. **6**. Subsequently, we assume that the limiting DFT is handled this way. The DFT given by Eq. **6** is exact, so it may be used to check an FFT program for any N.

We have thus obtained directly for the complex exponential a closed-form DFT in which N may be any positive

The publication costs of this article were defrayed in part by page charge payment. This article must therefore be hereby marked "*advertisement*" in accordance with 18 U.S.C. §1734 solely to indicate this fact.

Abbreviations: DFT, discrete Fourier transform; FFT, fast Fourier transform; FIT, Fourier integral transform.

integer. If the FFT is used, its common implementation (the radix-2 form) requires that N be of the form 2^i, where i is a positive integer, and that n be an integer. To simplify comparison between our analytical expressions and the FFT, we make such restrictions in the numerical examples below. The general symmetry properties of the DFT (1–8) are readily verified for Eq. **6**—namely that if the function to be transformed is real (α real), then

$$H_N(N-n) = H_N^*(n) \qquad \text{Im } \alpha = 0, \qquad [8]$$

so Re $H_N(n)$ is symmetric and Im $H_N(n)$ is antisymmetric about the midpoint $n = N/2$ (for N even). For any α, the midpoint value is

$$H_N(N/2) = \Delta t\left[\frac{1-e^{-\alpha N\Delta t}}{1+e^{-\alpha\Delta t}} - \frac{1}{2}\right]. \qquad [9]$$

Transition to the FIT can be made from Eq. **6** by letting $N\Delta t \to \infty$ as $\Delta t \to 0$ and assuming Re $\alpha > 0$ to guarantee convergence. By expanding the denominator to lowest order in $\alpha\Delta t$ and then letting $\Delta t \to 0$, one readily finds the limit as the *relaxation function*

$$H_N(n) \to R(\omega) = \frac{1}{\alpha + j\omega}, \qquad [10]$$

where $R(\omega)$ is the integral transform of the complex exponential in Eq. **1** and ω is now continuous.

Exponential decay. With α in Eq. **1** real and positive, we have pure exponential decay. With appropriate units for α and Δt, the time step Δt can be measured in units of $1/\alpha$; then we can set $\alpha = 1$ so that Eq. **6** becomes

$$H_N(n) = \Delta t\left[\frac{1-e^{-N\Delta t}}{1-e^{-\Delta t}e^{-2\pi jn/N}} - \frac{1}{2}\right]. \qquad [11]$$

The midpoint value and integral-transform limit are obtained by setting $\alpha = 1$ in Eqs. **9** and **10**. Our analytical example agrees with that computed numerically by the FFT in chapter 9.4 of Brigham (2).

For N large and Δt small (but finite), it is interesting to calculate from Eqs. **9** and **10** the ratio of the midpoint DFT to the FIT at midpoint angular frequency, calculated from Eq. **3** as $\pi/\Delta t$. One finds that as $\Delta t/N \to 0$,

$$\frac{H_N(N/2)}{R(\pi/\Delta t)} \approx \left(\frac{\pi}{2}\right)^2 + \left(\frac{\Delta t}{2}\right)^2 \to 2.46740. \qquad [12]$$

For zero frequency ($n = 0$, so $\omega = 0$), and in the limit of large N, Eqs. **6** and **10** with $\alpha = 1$ show that the DFT overpredicts the transform compared with the FIT by an amount that increases as Δt increases. In Brigham's comparison of the DFT and FIT for exponential decay (equation 2, chapter 9.1 of ref. 2), the DFT values presented graphically are numerical FFT values and there is no discussion of why the DFT and FIT are discrepant or of how the discrepancy depends upon N and Δt.

In Fig. 1 the DFT has been evaluated for $\Delta t = 1$ at integer values of n for $N = 32$ and 64, powers of 2 for which the FFT might be used. Also, n has been stopped at $N - 1$, as in an FFT. The large-N limit is actually the result for $N = 128$, which takes no longer to calculate for each n value than for $N = 32$. The symmetry of Re H_N and antisymmetry of Im H_N about $N/2$ agree with Eq. **8** and show the effects of using finite N values to construct the transform. These so-called truncation effects are discussed in ref. 1, pp. 376–377, and in ref. 2, chapter 12.2.

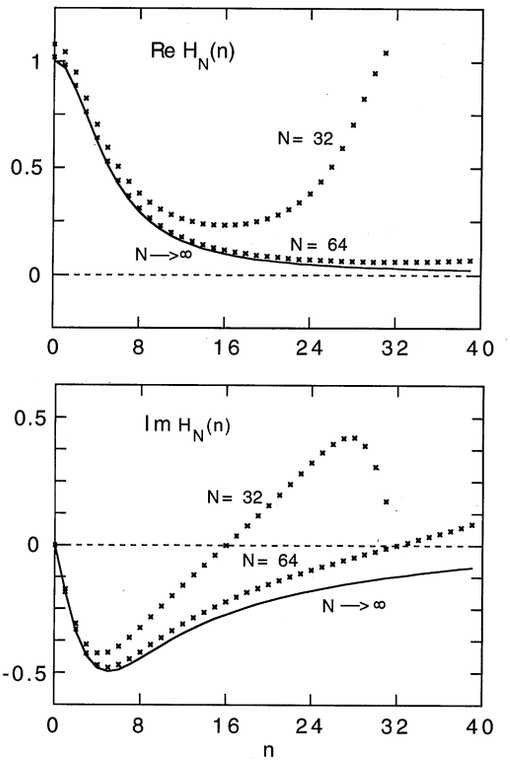

FIG. 1. DFTs (crosses) and FIT (line) for exponential decay, computed from analytic formulas. For $N = 32$ the results are the same as those in figures 9.17 (a) and (b) in ref. 2, obtained by using the FFT.

The dependence of the DFT on Δt is usually called *time-domain aliasing*, as in ref. 1, pp. 197–198, and in ref. 2, chapters 5.3 and 5.4. According to the Nyquist sampling criterion discussed in ref. 2, chapter 5.4, if $\Delta t < 1/(2N)$ the effects of aliasing become negligible, provided that N is not too small. The ratio of DFT to FIT values at $n = N/2$ is given by setting $\alpha = 1$ in Eq. **9** and then multiplying by $[1 + (\pi/\Delta t)^2]$, which is the inverse of the real part of the FIT at the frequency corresponding to $n = N/2$. Numerical comparisons are shown in Fig. 2 for small N. The dashed line is the result of Eq. **12**. For N and Δt both small the DFT gives a *negative* real transform at $n = N/2$, quite different from the everywhere-positive real part of the FIT. This emphasizes the need for care in the limit process of deriving the FIT from the DFT, as described above Eq. **10**. Examples of the frequency-domain aliasing analyzed here are shown in figure

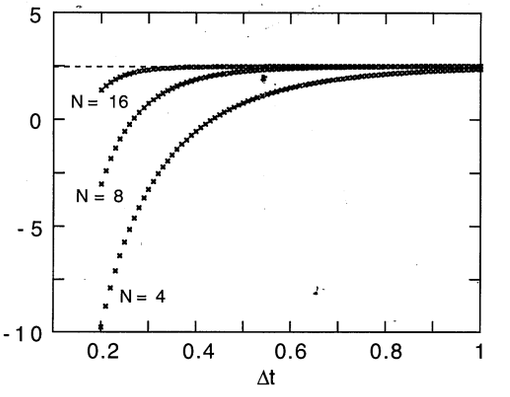

FIG. 2. Ratios of DFT to FIT for exponential decay at $n = N/2$ vs. Δt according to Eq. **12**.

9.3 in Brigham's book (2), but quantitative analysis of the aliasing is not provided.

Harmonic oscillator. Consider, in Eq. **1**, $\alpha = -j\,\omega_0$, a pure oscillator with frequency ω_0. A small positive real part, ε, has to be included in α to converge the geometric series for N large, as discussed below Eq. **1** and above Eq. **10**. Then we may let $\varepsilon \to 0$ to obtain the following well-known result for the FIT of a pure oscillator,

$$R(\omega) = j\frac{1}{\omega - \omega_0}, \qquad [13]$$

showing a simple pole at ω_0.

The analytical DFT of the oscillator can be simplified by substituting $\alpha = -j\omega_0$ in Eq. **6** and then expressing the complex exponentials in terms of half angles before converting to sines by using Euler's theorem. Thus

$$H_N(n, n_0) = \begin{cases} \Delta t\left\{\dfrac{e^{j\pi\left(n_0 - \frac{n_0 - n}{N}\right)}\sin(\pi n_0)}{\sin\left[\pi\dfrac{n_0 - n}{N}\right]} - \dfrac{1}{2}\right\} & n \neq n_0 \\ \Delta t\left[N - \dfrac{1}{2}\right] & n = n_0, \end{cases} \qquad [14]$$

where

$$n_0 = \frac{\omega_0 N \Delta t}{2\pi}, \qquad [15]$$

so that n_0 need not be an integer. The second line in Eq. **14** is obtained either by applying L'Hôpital's rule to the first line in Eq. **14** or from Eq. **7**. This DFT has no intrinsic dependence on Δt except through the scale factor inserted in Eq. **2** to produce the FIT limit and the conversion Eq. **15** between number and frequency. Therefore, for the oscillator we set $\Delta t = 1$.

The symmetry of the DFT for real functions, Eq. **8**, does not hold for the oscillator, but there is a related symmetry,

$$H_N(N - n, N - n_0) = H_N^*(n, n_0), \qquad [16]$$

as may be verified by substituting in Eq. **14** and is exhibited in a numerical example below. When n_0 is an integer or half-integer, the oscillator DFT simplifies considerably, as can be shown by substituting the circular functions at multiples of π or $\pi/2$. For n_0 an integer, the oscillator DFT is

$$H_N(n, n_0) = \begin{cases} -\dfrac{1}{2} & n \neq n_0 \\ N - \dfrac{1}{2} & n = n_0. \end{cases} \qquad [17]$$

For n_0 a half-integer, such as 1/2 or 15/2, only the top line in Eq. **14** occurs. Then

$$H_N(n, n_0) = \frac{1}{2} + j\cot\left[\frac{\pi(n_0 - n)}{N}\right], \qquad [18]$$

so Im H_N is antisymmetric about n_0. As expected from the interpretation of a Fourier transform from time (t) domain to "frequency" (n) domain, Eqs. **17** and **18** show that in the latter the transforms depend on n most strongly near n_0, which is the value of n at the pole, as obtained from Eq. **15**.

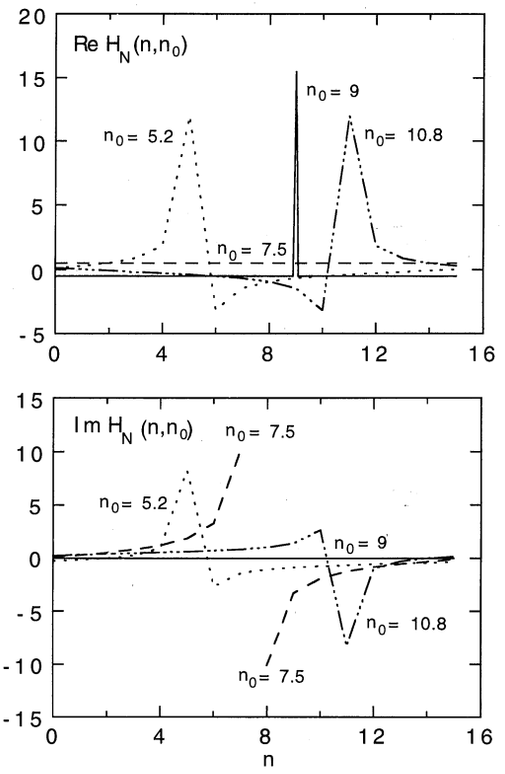

FIG. 3. Harmonic-oscillation DFT for $N = 16$ and various resonance values n_0. For $n_0 = 9$, the real part has a spike at $n = n_0$ and the imaginary part is zero everywhere.

To compute Eq. **14** numerically, real and imaginary parts can be immediately identified. For Fig. 3 we choose $N = 16$ and four values of n_0. For clarity of presentation, the DFT values for each n_0 are connected by line segments, except across the cotangent singularity for $n_0 = 7.5$. The symmetry Eq. **16** is made evident by choosing two n_0 values whose sum is N—namely, $n_0 = 5.2$ and $n_0 = 10.8$. Notice that for these n_0 values there is a broad distribution of DFT values about the oscillator frequency.

The two examples give the extremes of bounded exponential behavior, pure decay and pure oscillation. The more general case of the damped oscillator is just Eq. **6** for the DFT and Eq. **10** for the FIT. With damping, the latter does not have a pole at ω_0 but rather has nearly maximum magnitude if damping is small.

3. Frequency-to-Time Transform of the Relaxation Function

In the preceding section we showed how the DFT of a damped exponential in the time domain produces approximately a relaxation function in the frequency domain. Suppose, on the other hand, that in ω one has *exactly* a relaxation function—that is, $R(\omega)$ in Eq. **10** with α real. What is the inverse DFT in the time domain, t? As we will show, this transform can also be obtained in a form that improves comprehension of the DFT. The method of analysis differs sufficiently from the preceding that we give it in full.

Given $R(\omega)$ in Eq. **10**, we compute its inverse DFT over N points analogously to Eq. **2**,

$$h_N(t) = \begin{cases} 2\Delta f\,\mathrm{Re}\left[\left(\sum_{k=0}^{N-1}\dfrac{1}{1 + j(\omega_k/\alpha)}\,e^{j(\omega_k/\alpha)(\alpha t)}\right) - \dfrac{1}{2}\right] & t \geq 0 \\ 0 & t < 0, \end{cases} \qquad [19]$$

with t and a number n being related by

$$t = \frac{n}{N\,\Delta f}, \qquad [20]$$

analogously to Eq. **3**. In Eq. **20** the discrete frequencies, ω_k, are related to frequency increments, Δf, by

$$\omega_k = 2\pi\Delta f k. \qquad [21]$$

Our notation is that of Brigham (2), chapter 9. Eq. **19** shows that, in terms of variables αt and ω_k/α, the equation is invariant to scale changes in α. Therefore we set $\alpha = 1$ henceforth. From Eq. **19** the FIT is obtained in the limit of large N and $\Delta f \to 0$ as e^{-t}, as explained below in connection with Table 1.

To relate the discrete and integral transforms analytically, consider the derivative from Eq. **19** with $\alpha = 1$:

$$\frac{dh_N(t)}{dt} = -h_N(t) + U_N(t), \qquad [22]$$

where

$$U_N(t) = 2\pi\Delta f \sum_{k=0}^{N-1} e^{2\pi jk\Delta ft}. \qquad [23]$$

This series can be summed by using Eq. **5**, since it is a geometric series with multiplier

$$r = e^{2\pi j\Delta ft}, \qquad [24]$$

so that

$$U_N(t) = 2\pi\Delta f\,\mathrm{Re}\left[\frac{1 - e^{2\pi jN\Delta ft}}{1 - e^{2\pi j\Delta ft}}\right]$$

$$= 2\pi\Delta f \frac{\sin(\pi N\Delta ft)}{\sin(\pi\Delta ft)}\cos[\pi(N-1)\Delta ft]. \qquad [25]$$

We define the *overshoot function*, $O_N(t)$, which may be of either sign, as the difference between discrete and integral transforms:

$$O_N(t) \equiv h_N(t) - e^{-t}. \qquad [26]$$

For functions with discontinuities, the overshoot near a discontinuity is called the Gibbs phenomenon, as discussed in refs. 7 and 9. Fig. 4 shows $h_N(t)$, computed from Eq. **19** directly for $N = 32$ with $\Delta f = 1/N$, compared with the relaxation exponential in Eq. **26**, which is the FIT. Their difference is $O_N(t)$ in Eq. **26**. A similar figure but with only discrete points (since the FFT was used) is shown as figure 9.17(c) in ref. 2, but Brigham did not analyze the overshoot behavior.

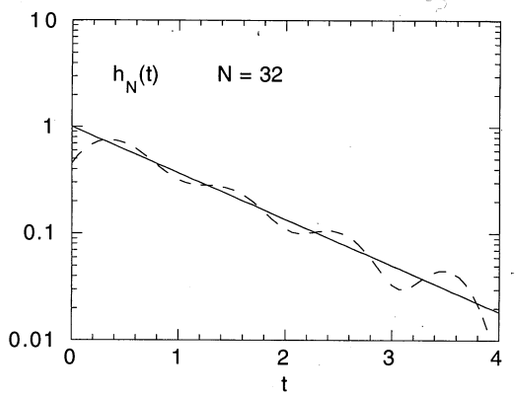

FIG. 4. Comparison on a logarithmic scale of the inverse DFT (dashed curve), calculated by using Eq. **19** with $\alpha = 1$ and $N = 32$, with the FIT (solid line) as functions of time, t, for relaxation function of Eq. **10**. The frequency step $\Delta f = 1/N = 1/32$.

Overshoot near the origin. The dependence of the overshoot near the origin on the discreteness of Δf (aliasing) and on the finite value of N (truncation) can be examined by making a Maclaurin expansion in t of $h_N(t)$ given by Eq. **19**. To our knowledge, there is no closed-form expression for the sum in Eq. **19**, even when $t = 0$. For the expansion we take successive derivatives with respect to t of $U_N(t)$ in Eq. **23**. The resulting sums can be expressed in closed form when $t = 0$. Thence

$$h_N(t) \approx h_N(0) + [h_N(0) + \Delta f](e^{-t} - 1)$$

$$+ 2\Delta f \sum_{n=0}^{\infty} s_{2n+1}\frac{t^{2n+1}}{(2n+1)!}\left(1 - \frac{t}{2n+2}\right), \qquad [27]$$

where the series coefficients are generated by recurrence,

$$s_{2n+1} = s_{2n-1} + (-1)^n(2\pi\Delta f)^{2n}\frac{(N-1/2)^{2n+1}}{2n+1},$$

$$s_1 = 2\pi\Delta fN, \qquad [28]$$

in which a very close approximation to the sums of powers of integers has been used:

$$\sum_{k=0}^{N-1} k^n \approx \frac{\left(N - \frac{1}{2}\right)^{n+1}}{n+1}. \qquad [29]$$

For expansion Eq. **27**, which is most appropriate for t small, it remains to estimate $h_N(0)$. We may turn the tables on the usual practice and approximate the sum in Eq. **19** for $t = 0$ by an integral, using the trapezoid rule. Thus

$$h_N(0) = 2\Delta f\left[\left(\sum_{k=0}^{N-1}\frac{1}{1+\omega_k^2}\right) - \frac{1}{2}\right]$$

$$\approx 2\Delta f\left[\frac{\int_0^{\omega_{N-1}}\frac{d\omega}{1+\omega^2}}{2\pi\Delta f} + \frac{1}{2}\left(1 + \frac{1}{1+\omega_{N-1}^2}\right) - \frac{1}{2}\right], \qquad [30]$$

in which the divisor of the integral relates unit steps of k to increments in ω according to Eq. **21**, and endpoint values of the integrand have been included. The integral is elementary and the resulting arctangent function can be written so that the behavior for large ω_{N-1} is evident, to obtain the trapezoid-formula estimate of the DFT at the time origin, $h_{\mathrm{trap}N}(0)$, as

$$h_N(0) \approx h_{\mathrm{trap}N}(0) \equiv \frac{1}{2} - \frac{1}{\pi}\tan^{-1}\left(\frac{1}{\omega_{N-1}}\right) + \frac{\Delta f}{1+\omega_{N-1}^2}. \qquad [31]$$

Correspondingly, we write for the overshoot near the origin

$$O_{\mathrm{trap}N}(t) = h_{\mathrm{trap}N}(t) - e^{-t}, \qquad [32]$$

in which the trapezoid approximation for $h_N(t)$ is obtained by substituting Eq. **31** into Eq. **27**.

As with other examples of the Gibbs overshoot, such as in refs. 7 and 9, the behavior of this overshoot at the origin depends sensitively on the relation between N and Δf, as

summarized in Table 1. The first case, $\Delta f = 1/N$, produces very good agreement with exact numerically calculated values of $h_N(0)$, as shown in Fig. 5. In Table 1 the formula for $O_{\text{trap}N}(0)$ is obtained by expanding Eq. **31** through terms in $1/N$. The discrepancy between discrete and integral transforms does *not* disappear as $N \to \infty$, but it approaches a limiting value of -0.5502, so that the DFT at the origin is about 50% less than the FIT value of unity. Truncation, with N finite but $\Delta f \to 0$, leads to underestimating the transform by -1, since the DFT, Eq. **19**, is then zero.

Aliasing effects must be handled very carefully. Table 1 shows the result for $t = 0$ with Δf finite and $N \to \infty$, which produces one-half the FIT value of unity, thus $O_\infty(0) = -1/2$. On the other hand, if for $t > 0$ one makes in Eq. **19** with $\alpha = 1$ the integral approximation to the sum, one obtains by contour integration $h_\infty(t) = e^{-t}$, so $O_\infty(t \to 0) = 0$, that is, exact agreement with the integral transform, the last row in Table 1. Thus, like the classical Gibbs phenomenon, the overshoot depends upon the order of taking limits.

Overshoot for large N. In the limit of large N the overshoot may be estimated as the integral of $U_N(t)$ given in Eq. **25**, with $O_N(t)$ as its integral in the large-N limit. Then $O_N(t)$ can be approximated in terms of the sine integral, Si (entry 5.2 in ref. 10), as $O_N(t) \approx O_{iN}(t)$, where

$$O_{iN}(t) \equiv \frac{1}{\pi}\,\text{Si}(2\pi N\Delta f t)$$

$$= -\frac{1}{\pi}\,[f(2\pi N\Delta f t)\cos(2\pi N\Delta f t) + g(2\pi N\Delta f t)\sin(2\pi N\Delta f t)] \qquad [33]$$

in terms of auxiliary functions f and g, equations 5.2.6 and 5.2.7 in ref. 10. The overshoot is an extremum for t such that $U_N(t)$ is zero. From Eq. **25**, for N large the Mth extremum occurs at integer n in Eq. **20**—namely, $n = M$, and at extrema the time is

$$t = t_M = \frac{M}{2N\Delta f} \qquad M = 1, 2, \ldots \qquad [34]$$

In this large-N approximation, overshoot extrema therefore depend only on f, and for this we use a rational approximation with an error of $<2 \times 10^{-4}$, equation 5.2.36 in ref. 10. This produces

$$O_{iN}(t_M) = \frac{(-1)^M}{\pi} f(M\pi) \approx \frac{0.1013(-1)^M}{M}\,\frac{1 + (0.7337/M^2) + (0.0253/M^4)}{1 + (0.9189/M^2) + (0.07353/M^4)}. \qquad [35]$$

Table 1. Overshoot at the origin, $t = 0$, of the frequency-to-time DFT of the relaxation function, estimated by Eq. **31** as a function of number of points in the transform, N, and frequency increment, Δf

Effect	N	Δf	$O_{\text{trap}N}(0)$
—	N	$1/N$	$-0.5502 - \dfrac{0.033}{N}$
Truncation	Finite	$\to 0$	-1
Aliasing	$\to \infty$	Finite	$-1/2$
($t = 0$)	$\to \infty$	Finite	0

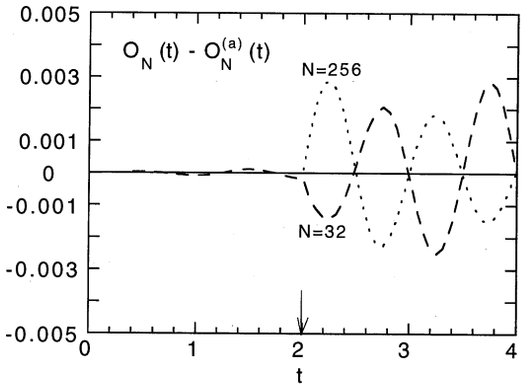

FIG. 5. Comparison of overshoots for the inverse DFT as functions of time, t, for relaxation function, Eq. **10** for $N = 32$ (dashed) and $N = 256$ (dotted). Shown is the difference between exact overshoot, $O_N(t)$, and approximate overshoot, $O_N^{(a)}(t)$, estimated by Eq. **27** for $t \le 2$ and by Eq. **33** for $t > 2$, as discussed in the text and indicated by the arrow at $t = 2$. For $t \le 2$ the two curves are unresolved. The frequency steps $\Delta f = 1/N$.

These results are independent of Δf and of N, except for the simple N dependence of t_M in Eq. **34** and omitted terms in $1/N$ and higher when $O_N(t)$ is approximated by $O_{iN}(t)$. Therefore we have a genuine Gibbs phenomenon as described (6, 8). Since the width of each over- or undershoot decreases as $1/N$ and its value becomes independent of N, its area decreases as $1/N$. Therefore, if the time jitter is more than about $1/(N\Delta f)$ the overshoot effects become unresolved and one nearly recovers the integral transform, e^{-t}. The first maximum of $O_N(t)$ occurs at $t_1 \approx 1/(2N\Delta f)$, where the overshoot in the integral approximation is

$$O_{iN}(t_1) \approx 0.0895. \qquad [36]$$

In Fig. 5 we show the difference between the exact overshoot and its approximations, Eqs. **27** and **33**, for a small N value, $N = 32$, as well as for $N = 256$, both with $\Delta f = 1/N$. For $t \le 2$ we use $O_N^{(a)}(t) = O_{\text{trap}N}(t)$ with 10 terms in the series Eq. **28**, while for $t > 2$ $O_N^{(a)}(t) = O_{iN}(t)$. Only near this changeover point is the discrepancy with the exact overshoot >0.003, and it can be decreased by taking more terms in the expansion and using it for larger t. In this example, all the overshoot extrema are predicted to within 3×10^{-4}.

The work reported here was supported in part by U.S. Department of Energy Grant DE-FG05-88ER40442.

1. Bracewell, R. N. (1986) *The Fourier Transform and Its Applications* (McGraw-Hill, New York), 2nd Ed., revised.
2. Brigham, E. O. (1988) *The Fast Fourier Transform and Its Applications* (Prentice–Hall, Englewood Cliffs, NJ).
3. Jerri, A. J. (1992) *Integral and Discrete Transforms with Applications and Error Analysis* (Dekker, New York), Section 4.16.
4. Kunt, M. (1986) *Digital Signal Processing* (Artech House, Norwood, MA).
5. Oppenheim, A. V. & Schafer, R. W. (1989) *Discrete-Time Signal Processing* (Prentice–Hall, Englewood Cliffs, NJ).
6. Roberts, R. A. & Mullis, C. T. (1987) *Digital Signal Processing* (Addison–Wesley, Reading, MA).
7. Thompson, W. J. (1992) *Computing for Scientists and Engineers* (Wiley–Interscience, New York).
8. Weaver, H. J. (1983) *Applications of Discrete and Continuous Fourier Analysis* (Wiley–Interscience, New York).
9. Thompson, W. J. (1992) *Am. J. Physiol.* **60**, 425–429.
10. Abramowitz, M. & Stegun, I. A. (1964) *Handbook of Mathematical Functions* (Dover, New York).